Indonesian Journal of Chemical Research

http://ojs3.unpatti.ac.id/index.php/ijcr Indo. J. Chem. Res., 14 (1), 1-9, 2026

Synthesis of Activated Carbon from PET (Polyethylene Terephthalate) Plastic Waste with Fe_3O_4 Composite as Adsorbent for Methylene Blue

Ninik Andriani[1*], Kholidah[2]

[1]Department of Chemistry, Faculty of Science and Technology, Universitas Islam Negeri Walisongo Semarang, Walisongo Street no. 3-5 Semarang. 50185, Indonesia
[2]Department of Chemistry, Faculty of Science and Technology, Universitas Islam Negeri Walisongo Semarang, Walisongo Street no. 3-5 Semarang. Indonesia
[*]*Corresponding Author: ninikandri2310@gmail.com*

Received: October 2025
Received in revised: January 2026
Accepted:May 2026
Available online: May 2026

Abstract

The purpose of this research is to produce an activated carbon composite from PET (Polyethylene Terephthalate) plastic waste combined with Fe_3O_4 for methylene blue dye wastewater treatment. Activated carbon was produced by carbonizing PET plastic, followed by physical activation at 850°C for 25 minutes and chemical activation by soaking in 4M KOH for 2 hours. Activated carbon–Fe_3O_4 composite was synthesized by coprecipitation with mass ratios of 1:1 (composite 1), 3:2 (composite 2), and 2:1 (composite 3). XRD and SEM were used to analyze the activated carbon, and the best-performing composite was further characterized by XRD and SEM-EDX mapping. The composite contains a crystalline phase, likely originating from Fe_3O_4. The composite's morphology consists of fine, high-surface-area particles. The detection of Fe and O peaks in the elemental analysis verified the existence of Fe_3O_4 within the sample. The highest adsorption capacity was achieved by composite 2, reaching 3.244 mg/g under optimum conditions at pH 7 for 30 minutes, and was best fit by the pseudo-second-order adsorption kinetic model. The synthesis of the activated carbon–Fe_3O_4 composite enhances the adsorption capacity for methylene blue and facilitates separation using an external magnet.

Keywords: PET (Polyethylene Terephthalate) Plastic, *Fe_3O_4, Adsorpstion and methylene Blue.*

INTRODUCTION

As time elapses, the need for clothing continues to increase, and the textile industry is crucial to fulfill these needs. Textile manufacturing involves dyeing, but most textile industries use synthetic dyes. Methylene blue is one such synthetic dye, which can cause cyanosis if inhaled and skin irritation (Wismayanti et al., 2015). In the dyeing process, dyes are not fully absorbed by the fabric, resulting in high levels of dye residue in the effluent (Ristianingsih et al., 2020). The dye waste produced by the textile industry is highly hazardous to the environment if disposed of directly into water bodies, as it obscures the water's surface, preventing sunlight from penetrating. This negatively impacts the aquatic ecosystem, ultimately leading to environmental damage (Susanti et al., 2022).

Methylene blue adsorption can be performed using activated carbon. Activated carbon mainly consists of carbon atoms and has a high surface area, enabling strong adsorption. Activated carbon can be produced from carbon-based sources such as biomass, vegetable oils and waste (Rafli et al., 2021). Among these, polyethylene terephthalate (PET) waste represents a potential alternative source of carbon material, with a high carbon content (over 60 wt.%) (Yuan et al., 2020). Then, PET plastic can be used only once and discarded as waste, thereby negatively impacting the environment through pollution (Mendoza-carrasco et al., 2016).

The adsorption process is limited by difficulties in separating the adsorbent and adsorbate. To overcome this, activated carbon can be composited with magnetite (Lestari et al., 2021). Magnetite (Fe_3O_4) is an iron oxide compound with the strongest magnetic properties. The combination of activated carbon with magnetite makes the composite responsive to an external magnetic field, thereby simplifying the

separation of the adsorbent from the adsorbate. In addition, combining activated carbon with magnetite can increase adsorption capacity by leveraging the adsorption properties of the constituent materials (Suryani et al., 2024). The activated carbon-Fe_3O_4 composite provides an adsorbent with a broad surface area and high porosity, and it exhibits superparamagnetic properties, enabling magnetic separation with an external magnet (Lestari et al., 2021).

METHODOLOGY

Materials and Instrumentals

The study utilized various laboratory equipment, such as glassware, oven, porcelain, analytical balance, stopwatch, thermometer, 100 mesh sieve, desiccator, universal pH, vial bottle, furnace (Thermo Scientific Thermolyne), magnetic stirrer (Cimarec), shaker (DLAB), centrifuge (PLC Series), UV-Vis Spectrophotometer (Thermo Scientific Orion AquaMate 8100), X-Ray Diffraction (XRD) (Panalytical X'pert 3 Powder), and Scanning Electron Microscope-Energy Dispersive X-Ray Mapping (SEM-EDX Mapping) (Phenom Pro X with EDX).

The materials utilized in this study were PET (Polyethylene Terephthalate) plastic waste from Le mineral, Aqua and Kh-Q brand mineral water bottles, acetone (C_3H_6O, Merck, p.a), 4M potassium hydroxide (KOH, Merck, p.a), iron(III) chloride hexahydrate ($FeCl_3.6H_2O$, Merck, p.a), iron(II) sulfate heptahydrate ($FeSO_4.7H_2O$, Merck, p.a), 25% ammonium hydroxide (NH_4OH, Merck, p.a), 0.5 M sodium hydroxide (NaOH, Merck, p.a), 0.5 M hydrochloric acid (HCl, Merck, p.a), methylene blue ($C_{16}H_{18}N_3SCl$, Merck, p.a) and distilled water.

Methods

Activated Carbon Synthesis

PET plastic waste was washed, chopped into small pieces, and subsequently dried. The dried PET plastic waste was then carbonized at 550°C for 15 minutes. The PET carbon was ground and passed through a 100-mesh sieve (Pham, 2023). The PET carbon powder was treated with acetone for 24 hours, dried at room temperature, and calcined at 850°C for 25 minutes (Cundari et al., 2016; Pham, 2023). The carbon was then activated in a 4M KOH solution for 2 hours. After that, it was filtered, and the pH was neutralized by rinsing with distilled water, then dried for 3 hours in an oven at 110°C (Oko et al., 2021).

Proximate Analysis of PET Carbon and Activated Carbon

Determination of Moisture Content

Porcelain crucibles were heated to 110°C for 30 minutes, cooled in a desiccator for 15 minutes, and weighed to determine their empty weight. Each 1 g of carbon and activated carbon was placed into porcelain crucibles of known mass. The crucibles were heated to 110°C for 2 hours, cooled in a desiccator for 30 minutes, and weighed to record the final mass. Repeated heating was carried out until a constant weight was obtained (Susmanto et al., 2020).

The moisture content can be quantitatively evaluated using the equation below (Susmanto et al., 2020):

$$\text{Moisture content (\%)} = \frac{W_2 - W_3}{W_2 - W_1} \text{x} 100\% \quad (1)$$

Determination of Ash Content

Crucibles were preheated to 110°C for 30 minutes, cooled, and weighed to determine their empty weight. Then, 1 g of carbon and 1 g of activated carbon were separately loaded into crucibles, which were heated in a furnace at 600°C for 2.5 hours to convert the samples to ash. After cooling in a desiccator for 30 minutes, the crucibles were weighed (Susmanto et al., 2020).

The ash content is quantified using the following equation (Susmanto et al., 2020):

$$\text{Ash content (\%)} = \frac{W_3 - W_1}{W_2 - W_1} \text{x} 100\% \quad (2)$$

Determination of Volatile Matter Content

Porcelain crucibles were first heated in an oven at 110°C for 30 minutes, cooled, and weighed to determine their empty mass. Subsequently, 1 g of carbon and 1 g of activated carbon were each placed into a crucible and heated in a furnace at 700°C for 2.5 hours to remove volatile matter. The crucibles were then cooled in a desiccator for 30 minutes and weighed to obtain the final mass (Susmanto et al., 2020).

The volatile matter is determined using the following formula (Susmanto et al., 2020):

$$\text{Volatile matter content (\%)} = \frac{W_2 - W_3}{W_2 - W_1} \text{x} 100\% - \%\text{moisture content} \quad (3)$$

W_1 : The mass of the empty crucible
W_2 : The mass of the crucible and sample before heating
W_3 : The mass of the crucible and sample after heating

Determination of Fixed Carbon Content

The fixed carbon content is obtained from the difference between the percentage of initial mass of carbon or activated carbon (100%) and the percentage of water content, ash content, and volatile matter content.

The carbon content is quantified using the following formula:

Fixed carbon content (%)
= 100% - (%moisture content + %ash content + % volatile matter content) (4)

Synthesis of a Composite of PET Activated Carbon with Magnetite Fe_3O_4

PET activated carbon-Fe_3O_4 composite was prepared using mass ratios of activated carbon and Fe_3O_4 of 1:1 (composite-1), 3:2 (composite-2), and 2:1 (composite-3). The initial step in the synthesis of each composite was to add 200 mL of distilled water to the activated carbon and stir it with a magnetic stirrer while heating to 70°C. Then, 200 mL of a solution of $FeCl_3.6H_2O$ and $FeSO_4.7H_2O$ in a 2:1 mole ratio was added to the solution. Next, 100 mL of 25% NH_4OH was added dropwise to the mixture of activated carbon and Fe_3O_4 to obtain a composite precipitate. After that, the precipitate was filtered and rinsed with demineralized water to adjust its pH to neutral and dried in an oven at 100°C for 3 hours (Reknosari et al., 2020; Suryani et al., 2024).

Adsorption Performance Comparison of PET Carbon, PET Activated Carbon, and Composites-1, 2, and 3 for Methylene Blue Dye

Each 0.1 g sample of PET carbon, PET activated carbon, and composites 1, 2 and 3 was added to an Erlenmeyer flask containing 20 mL of 20 ppm methylene blue solution. The mixtures were agitated at 300 rpm for 30 minutes using a shaker. After that, the solution was centrifuged to separate the filtrate from the solid residue. The filtrate obtained was then measured for the concentration of remaining methylene blue using a UV-Vis spectrophotometer (Meilianti, 2018). The adsorbent with the highest adsorption capacity was identified as the best composite and used for the pH and contact time optimization step.

The adsorption capacity (Qe) is calculated using the following equation:

$$Qe = \frac{(Co - Ce)}{m} x\ V \quad (5)$$

pH optimization

0.1 g of the best composite was suspended in 20 mL of a 20 ppm methylene blue solution and stirred at 300 rpm for 30 minutes at pH 4, 5, 6, 7, 8, 9, and 10, adjusted with 0.5 M HCl and 0.5 M NaOH. The mixture was then centrifuged, and the absorbance of the resulting supernatant was measured using a UV-Vis spectrophotometer. The adsorption capacity (Qe) is quantified using the following formula in equation 5.

Contact Time Optimization

A mass of 0.1 g of the best composite was added to 20 mL of a 20 ppm methylene blue solution. Next, the pH was adjusted to the optimum pH. The suspension was agitated on a shaker at 300 rpm for varying contact times of 1, 5, 10, 20, 30, 40, 50, 60, 90, and 120 minutes. Following agitation, the mixture was centrifuged to separate the supernatant from the solid phase, and the supernatant absorbance was measured using a UV-Vis spectrophotometer. The adsorption capacity (Qe) is quantified using the following formula in equation 5.

Determination of The Adsorption Kinetic Model

Pseudo-first-order and pseudo-second-order models were applied to investigate the adsorption kinetics of methylene blue onto the activated carbon-Fe_3O_4 composite. The pseudo-first-order adsorption kinetic curve was obtained by plotting the contact time on the x-axis and log Qe-Qt on the y-axis. Meanwhile, for the pseudo-second-order kinetic curve, the contact time was plotted on the x-axis, and the y-axis showed the t/Qt value.

The equation for the pseudo-first-order adsorption model is found in equation:

$$\log (qe - qt) = \log qe - \frac{K_1}{2{,}303} t \quad (6)$$

The pseudo-second-order adsorption model is represented by the following equation:

$$\frac{t}{q_t} = \frac{1}{k_2 qe^2} + \frac{1}{qe} t \quad (7)$$

RESULTS AND DISCUSSION

Synthesis and proximate analysis of activated carbon

The preparation of activated carbon derived from PET plastic waste begins with the carbonization stage, which aims to form a pore structure and to produce fixed carbon by evaporating non-carbon elements (Urhasanah et al., 2024). The PET carbon produced in this process is a fine black powder, with a yield of 20%. Physical activation at 850°C for 25 minutes is expected

to produce activated carbon with a perfectly activated pore structure (Pham, 2023). Meanwhile, chemical activation with 4 M KOH solution is expected to increase the adsorption capacity of activated carbon (Oko et al., 2021). This is because KOH is a strong

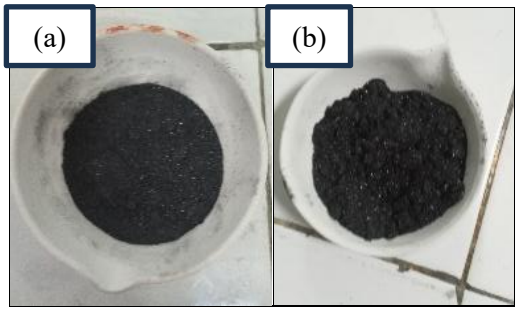

Figure 1. (a) carbon and (b) activated carbon

base and hygroscopic, allowing it to bind water during the activation process. In addition, the activator solution can dissolve impurities in the pores of the activated carbon (Sailah et al., 2020). The combination of these two activation processes increases carbon's adsorption capacity by increasing the number of pores (Urhasanah et al., 2024). The resulting activated carbon is a fine powder with a darker black color than the carbon before activation (Figure 1).

The quality improvement of activated carbon compared to unactivated carbon was determined using proximate analysis, with the results shown in Table 1. Based on Table 1, both characteristics meet SNI criteria, and the activation process can improve the quality of activated carbon. This is indicated by decreases in water, ash, and volatile matter content, and an increase in fixed carbon content. The chemical reactions that occur during the chemical activation process are written in reactions (1), (2), and (3) (Hanum et al., 2017).

$$4KOH_{(aq)} + C_{(s)} \rightarrow 4K^{+}_{(aq)} + CO_{2(g)} + 2H_2O_{(l)} \quad (1)$$

$$6KOH_{(aq)} + 2C_{(s)} \rightarrow 2K^{+}_{(aq)} + 3H_{2(g)} + 2K_2CO_{3(aq)} \quad (2)$$

$$4KOH_{(aq)} + 2CO_{2(s)} \rightarrow 2K_2CO_{3(aq)} + 2H_2O_{(l)} \quad (3)$$

The proximate analysis of carbon and activated carbon is summarized in Table 1.

Table 1. Results of proximate analysis of carbon and activated carbon

Properties	Content (%)		
	Carbon	Activated Carbon	SNI
Moisture	0.8917	0.5288	max.15
Ash	4.6556	0.5621	max.10
Volatile matter	8.0315	7.9416	max.25
Fixed carbon	86.4213	89.9768	min.65

Synthesis and characterization of activated carbon-Fe_3O_4 composite

Activated carbon-Fe_3O_4 composites were synthesized through the coprecipitation technique, using $FeCl_3.6H_2O$ and $FeSO_4.7H_2O$ precursors in a molar ratio of 2:1. The chemical reaction that occurs in the formation of Fe_3O_4 is shown in the reaction (4) (Adhim, 2018).

$$2Fe^{3+} + Fe^{2+} + 8OH^{-} \rightarrow Fe_3O_4 + 4H_2O \quad (4)$$

Magnetite has reliable magnetic properties, facilitating the separation of adsorbents from adsorbates (Lestari et al., 2021). Furthermore, Fe_3O_4 is a particle with a large surface area, so when composited with activated carbon, it can increase adsorption capacity by combining the adsorption properties of activated carbon and Fe_3O_4 (Fatmawati et al., 2024). The composition of the activated carbon and Fe_3O_4 in the composite influences the composite's adsorption capacity. Composites with higher activated carbon content will give a more intense black color (Figure 2), indicating a decrease in Fe_3O_4 content.

XRD and SEM were used to analyze the activated carbon, and the best-performing composite was further characterized by XRD and SEM-EDX mapping. The best-performing composite is the one with the highest methylene blue adsorption capacity, as indicated by the adsorption test results in Table 3. The X-ray diffraction patterns of activated carbon and

Figure 2. The synthesis result of Composite-1, 2, and 3

composite-2, shown in Figure 3, indicate that activated carbon has an amorphous phase, with broad peaks at 2θ values of 23.68° and 42.58°. The crystalline phase of Fe_3O_4 is present in composite-2, as indicated by 2θ diffactogram peaks at 30.32°; 35.66°; 43.30°; 57.37° and 63.00°, which correspond to the Miller indices [220], [311], [400], [511], and [440], respectively These angles exhibit diffraction patterns similar to

those of Fe_3O_4 synthesized by Fisli *et al*. (2012) with the highest 2θ diffraction peaks at 30.32°, 35.32°, 43.54°, 57.44°, and 62.98°. This shows that magnetite particles of the Fe_3O_4 phase have been attached to the surface of the activated carbon structure. If more magnetite fraction is added to the composite, the intensity of diffraction peak obtained from magnetite will be higher (Arisa, Putri; Wirawan, Teguh; Tri Widodo, 2025).

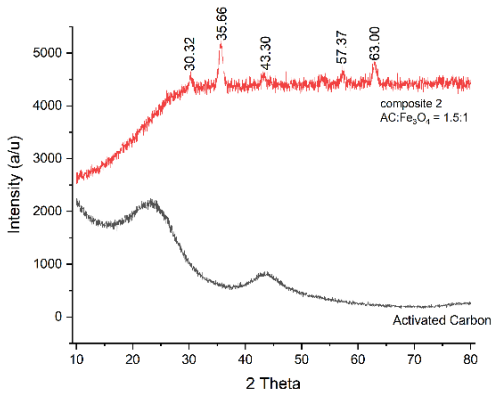

Figure 3. Diffractogram of activated carbon and composite-2

SEM characterization of activated carbon revealed lumps with a smooth, irregular surface and visible pores. At 5000x magnification, the surface of the activated carbon was clearly smooth and porous. This finding is similar to that of Pham (2023), who produced activated carbon from PET plastic waste, yielding irregular lumps with a relatively smooth morphology. This is also consistent with Aisyah *et al*. (2019), who observed pores in the surface morphology of activated carbon.

While SEM characterization of composite-2 showed small, smooth particles and more surface pores visible at 5000x magnification, this increased surface pore count increased the composite's adsorption capacity for methylene blue. Hariani *et al*. (2018) demonstrated that the morphology of activated carbon-Fe_3O_4 composites had an uneven surface, indicating the presence of Fe_3O_4. The SEM characterization data are shown in Figure 4.

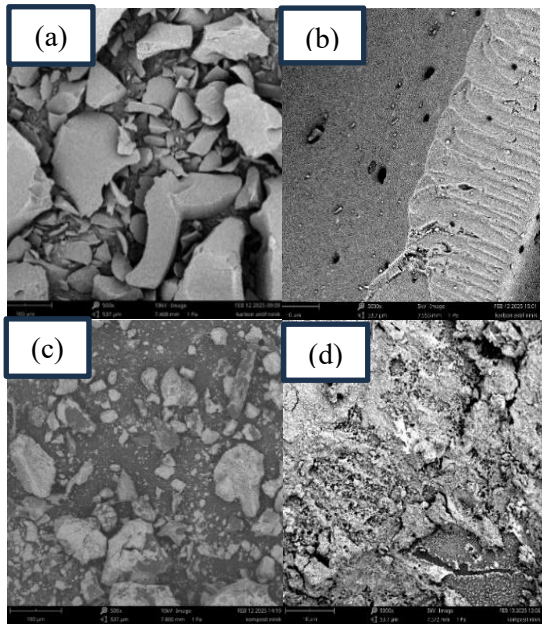

Figure 4. SEM images of (a) activated carbon (mag. 500x), (b) activated carbon (mag. 5000x), (c) composite-2 (mag. 500x), and (d) composite-2 (mag. 5000x)

The synthesis of composite-2 has been successfully carried out, reinforced by the results of Energy Dispersive X-Ray characterization, which shows the presence of Fe_3O_4 content with the detection of iron (Fe) and oxygen (O), as well as carbon (C) from activated carbon, with the percentages listed in Table 2.

The distribution of the constituent elements of composite-2 is shown in the elemental mapping analysis in Figure 5 which shows the elements distribution of Fe, O and C on its surface.

Table 2. Elemental compotition of composite-2

Elements	% Atom	% Mass
Iron (Fe)	17.86	46.73
Oxygen (O)	37.77	28.31
Carbon (C)	44.36	24.96

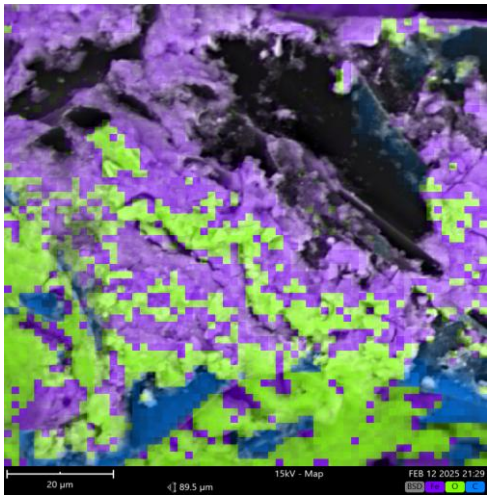

Figure 5. Elemental mapping analysis of composite-2 (Fe in purple, O in green, and C in blue color)

Adsorption of Methylene Blue Using Carbon, Activated Carbon and Composites-1, 2 and 3

To evaluate the performance of each adsorbent, an adsorption process was performed with all adsorbents, and their adsorption capacities were assessed. Table 3 shows that activated carbon exhibits better adsorption performance than unactivated carbon. This is because the activation process can enlarge the carbon's surface pores, thereby increasing its adsorption capacity. This is in line with the study by (Aisyah et al., 2019), which found that activated carbon has more surface pores than unactivated carbon.

Table 3. The capacity of adsorbents to adsorp methylene blue (mg/g)

Adsorbent	Adsorption capacity (mg/g)	Removal (%Q)
Carbon	2.4882	55,2513
Activated carbon	2.6378	58,5733
Composite-1	3.0079	66,7910
Composite-2	3.4961	77,6339
Composite-3	3.3648	74,7174

The addition of Fe_3O_4 to activated carbon has been shown to improve its adsorption performance, consistent with previous studies by (Pourzamani et al., 2017). A possible explanation is that Fe(III) salts have oxidizing properties, thus acting as activating agents for activated carbon (Do et al., 2011). Thus, the addition of Fe3O4 to activated carbon can produce pores that provide favorable adsorption conditions (Wu et al., 2023). Nevertheless, excessive addition of activated carbon resulted in diminished adsorption performance (T. T. Do et al., 2025).

The ability of each composite to be attracted to an external magnetic field shows that the higher the Fe_3O_4 content, namely in composite-1, brings out a greater magnetic field attraction ability, so that the separation ability is also better (Figure 6).

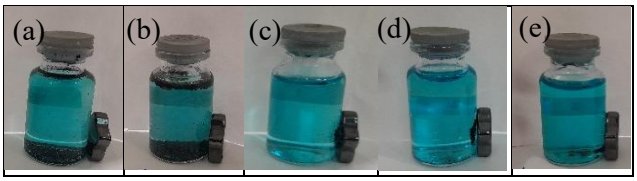

Figure 6. External magnetic attraction on adsorbents: (a) carbon, (b) activated carbon, (c) composite-1, (d) composite-2, and (e) composite-3

Effect of pH

The relationship between adsorbate pH and adsorption capacity is presented in Figure 7. The adsorption capacity increases with increasing pH from pH 5 to 7. At pH 7, the adsorption capacity reaches an optimum of 3.832 mg/g. This can occur because at pH 7, methylene blue can be directly adsorbed, as there is no competition between H^+ and OH^- ions (Dirgayanti et al., 2021). Then, the adsorption capacity decreases after pH 7. At pH < 7 (acid), two conditions occur, there is a very large number of H^+ ions and protonated methylene blue. The presence of excessive H^+ ions induces protonation on the adsorbent surface making it positively charged. Therefore, there is repulsion between the positively charged adsorbent and the cationic methylene blue, resulting in a low adsorption capacity (Pathania et al., 2017).

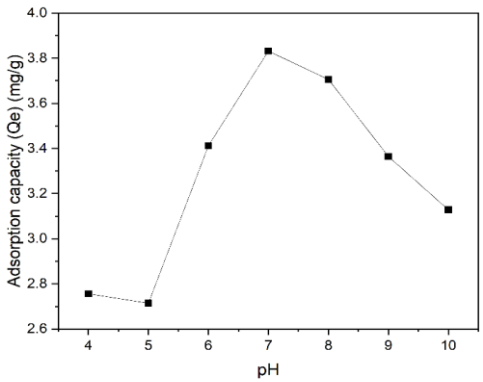

Figure 7. Effect of pH on adsorption

At pH > 7 (base), OH^- ions are abundant and methylene blue undergoes deprotonation. Under these conditions, the reduction in adsorption capacity is attributed to the interaction between OH^- ions in the solution and H+ ions released from methylene blue, making it difficult for the adsorbent to interact with methylene blue (Moniz et al., 2024).

Effect of Contact Time

Figure 8. demonstrates the correlation between contact time and adsorption capacity. At contact times of 1 to 30 minutes, adsorption capacity increases because longer contact times lead to more collisions between adsorbent and adsorbate, resulting in greater adsorption capacity. Meanwhile, at contact time between 60 and 120 minutes, the adsorption capacity declines. This reduction is attributed to methylene blue molecules occupying the adsorbent's active sites. This condition indicates that the adsorbent is saturated and the adsorption has reached equilibrium (Moniz et al., 2024). The optimum contact time in this study was 30 minutes, corresponding to an adsorption capacity (Qe) of 3.244 mg/g. These findings align with those of Hanum *et al*. (2017) who observed an optimal contact time of 30 minutes and a Qe value of 3.4 mg/g.

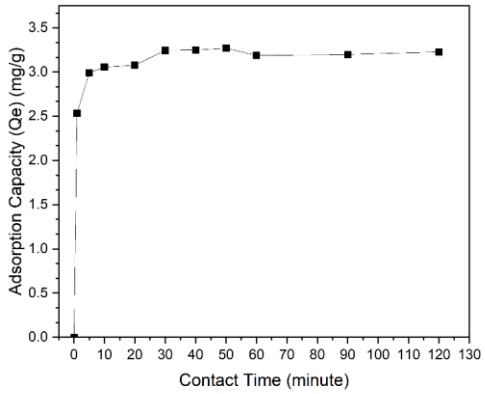

Figure 8. Effect of contact time on adsorption

Adsorption Kinetics

The theoretical Qe value, which is almost identical to the experimental Qe value, and the R^2 value, which is close to 1, are used as criteria for determining the appropriate adsorption kinetic model. As shown in Figure 9, the pseudo-first-order adsorption kinetic model produced a linear regression equation of y = -0.0103x – 0.4522 with an R^2 value of 0.3842. This equation can be employed to calculate the pseudo-first-order adsorption rate constant (K1) and the theoretical adsorption capacity (Qe). The K1 value obtained is 0.0154 min-1 and the Qe value is 0.5461 mg/g. Meanwhile, in the pseudo-second-order adsorption kinetic model, a linear regression equation, y = 0.30973x + 0.08236, was obtained with an R^2 value of 0.9998, as shown in Figure 10. Then the K2 value is 1.1538 g.mg-1.min-1 and the theoretical Qe is 3.229 mg/g. The adsorption constant value determined in the pseudo-second-order adsorption kinetics model is 1.1538 g.mg-1.min-1, meaning that for every adsorption process that lasts for one minute, there will be adsorption of 1.1538 mg of adsorbate for each gram of adsorbent (Nurhidayati et al., 2022).

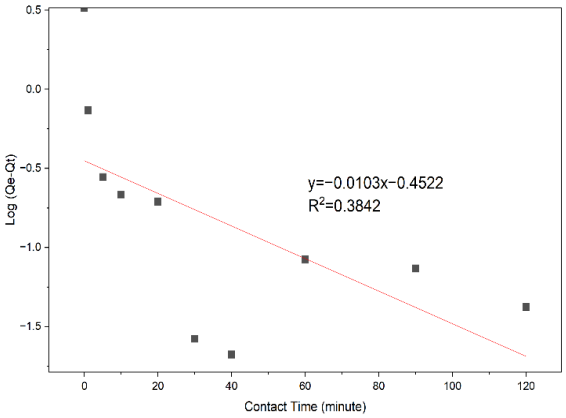

Figure 9. Pseudo-first-order kinetics adsorption model

Based on the result, it can be concluded that this study conforms to the pseudo-second-order kinetic model. This means that the adsorption rate at time t varies directly with the square of the adsorption capacity (Do et al., 2025). The results of the adsorption kinetic model analysis in this observation corroborate the research conducted by Do *et al*. (2025) as the Qe value obtained in the pseudo-second-order adsorption kinetic model closely approximates the experimental Qe value. The parameter data for each adsorption kinetic model are summarized in Table 4.

Table 4. Adsorption kinetic parameters

Adsorption kinetic model	Parameters		
Pseudo-first-order	Qe (mg/g)	K_1 (min $^{-1}$)	R^2
	0.5461	0.0154	0.3842
Pseudo-second-order	Qe (mg/g)	K_2 (g.mg^{-1}.min $^{-1}$)	R^2
	3.229	1.1538	0.9998

Qe experiment 3.244(mg/g)

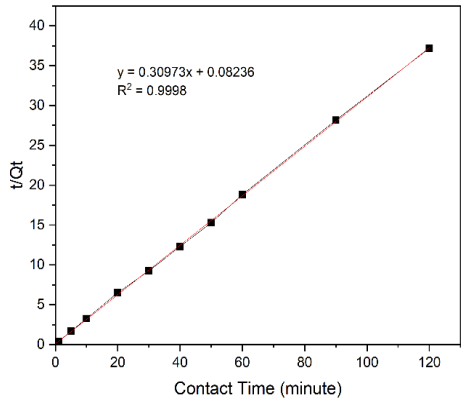

Figure 10. Pseudo second order kinetics adsorption model adsorption model

CONCLUSION

The addition of Fe_3O_4 into activated carbon derived from PET plastic significantly strengthens the material's ability to adsorp substances because it combines the adsorption capabilities of both activated carbon and Fe_3O_4. In addition, the addition of Fe_3O_4 allows the adsorbent to be separated efficiently from the adsorbate when subjected to an external magnetic field. The optimum conditions for methylene blue adsorption by the composite of PET-activated carbon with Fe_3O_4 were pH 7 and a contact time of 30 minutes at an initial concentration of 20 mg/L. The adsorption of methylene blue onto the PET-activated carbon-Fe_3O_4 composite follows a pseudo-second-order kinetic model.

REFERENCES

Adhim, M. S. (2018). Sintesis Nanopartikel Fe_3O_4 (Magnetit) dari Batu Besi Menggunakan Metode Kopresipitasi dengan Variasi PH *4*, 1–59.

Aisyah, S., Alimuddin, & Sitorus Saibun. (2019). Pengaruh Variasi Waktu Pada Kemampuan Adsorpsi Karbon Aktif dari Limbah Batang Pisang (Musa Paradisiaca L.) Terhadap Benzena. *Jurnak Atomik, 04 (2)* 90–95.

Arisa, Putri; Wirawan, Teguh; Tri Widodo, N. (2025). Adsorption of Methylene Blue Using Composite Fe_3O_4-Ihau Fruit Peel Powder (*Dimocarpus longan var. malesianus Leenh.*). *Indonesian Journal of Chemical Research*, *13*(2), 102–110.

Cundari, L., Yanti, P., & Syaputri, K. A. (2016). Pengolahan Limbah Cair Kain Jumputan Menggunakan Karbon Aktif dari Sampah Plastik. *Jurnal Teknik Kimia 22*(3), 26–33.

Dirgayanti, D. S., Koesnarpadi, S., & Hindryawati, N. (2021). Synthesis and characterization of Fe_3O_4-Activated carbon and it's application to adsorb methylene blue. *IOP Conference Series: Earth and Environmental Science*, *623*(1).

Do, M. H., Phan, N. H., Nguyen, T. D., Pham, T. T. S., Nguyen, V. K., Vu, T. T. T., & Nguyen, T. K. P. (2011). Activated Carbon/Fe_3O_4 Nanoparticle Composite: Fabrication, Methyl Orange Removal and Regeneration by Hydrogen Peroxide. *Chemosphere*, *85*(8), 1269–1276.

Do, T. T., Van, H. T., Pham, Q. H., & Nguyen, T. H. (2025). Adsorption of Ammonium from Aqueous Solution using Coffee Husk-derived Activated Charcoal Composite with Fe_3O_4 *Results in Surfaces and Interfaces*, *18*(February), 100471.

Fatmawati, R. A., Koesnarpadi, S., & Wirawan, T. (2024). Adsorpsi Ion Logam Kadmium (Ii) Menggunakan Magnetit (Fe_3O_4)-Arang Aktif dari Kulit Buah Tarap (Artocarpus odoratissimus). *Jurnal Atomik*. *9*(2), 110–119.

Fisli, A., Ariyani, A., Wardiyati, S., & Yusuf, S. (2012). Adsorben Magnetik Nanokomposit Fe_3O_4-Karbon Aktif untuk Meyerap Thorium. *Indonesian Journal of Material Science*, *13*(3), 192–197.

Hanum, F., Gultom, R. J., & Simanjuntak, M. (2017). Adsorpsi Zat Warna Metilen Biru dengan Karbon Aktif dari Kulit Durian Menggunakan KOH dan NaOH Sebagai Aktivator. *Jurnal Teknik Kimia USU*, *6*(1), 53.

Hariani, P. L., Faizal, M., Ridwan, Marsi, & Setiabudidaya, D. (2018). Removal of Procion Red MX-5B from Songket's Industrial Wastewater in South Sumatra Indonesia using Activated Carbon-Fe_3O_4 composite. *Sustainable Environment Research*, *28*(4), 158–164.

Lestari, I., Prasetyo, E., & Gusti, D. R. (2021). Penggunaan Karbon Aktif Magnetit-Fe_3O_4 Sebagai Penyerap Zat Warna Remazol Yellow. *Journal BiGME*, *1*(1), 29–37.

Meilianti, M. (2018). Karakteristik Karbon Aktif dari Cangkang Buah Karet Menggunakan Aktivator H_3PO_4. *Jurnal Distilasi*, *2*(2), 1.

Mendoza-carrasco, R., Cuerda-correa, E. M., Alexandre-franco, M. F., & Fern, C. (2016). Preparation of High-quality Activated Carbon from Polyethyleneterephthalate (PET) Bottle Waste. Its Use in the Removal of Pollutants in Aqueous Solution. *Journal of Enviromental Management 181*, 522–535.

Moniz, L., Baunsele, A. B., Boelan, E. G., Kopon, A.

M., Maria, A. U., Tukan, M. B., & Komisia, F. (2024). Optimasi Adsorpsi Metilen Biru Memanfaatkan Sabut Buah Lontar Teraktivasi Asam. *Cakra Kimia (Indonesian E-Journal of Applied Chemistry) 12*, 17–31.

Nurhidayati, I., Mellisani, B., Puspita, F., & Rahmawati Putri, F. A. (2022). Penentuan Isoterm dan Kinetika Adsorpsi Ion Besi oleh Sedimen Sebagai Adsorben. *Warta Akab*, *46*(1).

Oko, S., Mustafa, M., Kurniawan, A., & Norfitria, L. (2021). Pembuatan Karbon Aktif dari Limbah Plastik PET (Polyethylene terephthalate) Menggunakan Aktivator KOH. *Metana*, *17*(2), 61–68.

Pathania, D., Sharma, S., & Singh, P. (2017). Removal of Methylene Blue by Adsorption Onto Activated Carbon Developed from Ficus Carica Bast. *Arabian Journal of Chemistry*, *10*, S1445–S1451.

Pham, T. H. T. (2023). Synthesis of Activated Carbon from Polyethylene Terephthalate (PET) Plastic Waste and Its Application for Removal of Organic Dyes from Water. *Non-Metallic Material Science*, *5*(1), 27–37.

Pourzamani, H. R., Mengelīzadeh, N., & Jalil, M. (2017). Nitrate Removal from Aqueous Solutions by Magnetic Nanoparticle. *Journal of Environmental Health and Sustainable Development, Vol (2) Issue (1), 187-95.*

Rafli, Muhammad; Mega Wahyuni, Reza; Muna Zahiro, Nilna; Wayan Dasna, I. (2021). Magnetite-Activated Carbon Composite to Reduce Pollutant:Review. *Indonesian Journal of Chemical Research*, *9*(2), 69–79.

Reknosari, E., Wirawan, T., & Koesnarpadi, S. (2020). Phenol Adsorption Using Composite Adsorbent Fe_3O_4-Activated Charcoal Coffee Grounds. *Jurnal Kimia Mulawarman*, *18*(1), 30.

Ristianingsih, Y., Istiani, A., & Irfandy, F. (2020). Kesetimbangan Adsorbsi Zat Warna Metilen Blue dengan Adsorben Karbon Aktif Tongkol Jagung Terimpregnasi Fe_2O_3. *Jurnal Teknologi Agro-Industri*, *7*(1), 47–55.

Singkong, K., Sailah, I., Mulyaningsih, F., Ismayana, A., Puspaningrum, T., Adnan, A. A., & Indrasti, N. S. (2020). Kinerja Karbon Aktif Dari Kulit Singkong Dalam Menurunkan Konsentrasi Fosfat Pada Air Limbah Laundry. *Jurnal Teknologi Industri Pertanian*, *30*(2), 180–189.

Suryani, E., Destiarti, L., Program, N. *, Kimia, S., Matematika, F., Ilmu, D., Alam, P., Tanjungpura, U., Prof, J., & Nawawi, H. H. (2024). Sintesis Karbon Aktif Magnetik dari Tempurung Kelapa menggunakan Aktivator Soda Kue dengan Variasi Perbandingan Massa Karbon Aktif dan Oksida Besi. *Chimica et Natura Acta*, *12*(1), 19–27.

Susanti, I., Iqbal, R. M., Sholeha, N. A., & Putri, K. F. (2022). The Ecofriendly Biosorbent of Methylene Blue Using Banana Peels Waste. *Indo. J. Chem. Res.*, *10*(2), 93–96.

Susmanto, P., Yandriani, Y., Dila, A. P., & Pratiwi, D. R. (2020). Pengolahan Zat Warna Direk Limbah Cair Industri Jumputan Menggunakan Karbon Aktif Limbah Tempurung Kelapa pada Kolom Adsorpsi. *JRST (Jurnal Riset Sains Dan Teknologi)*, *4*(2), 77.

Urhasanah, A. N. N., Upriatna, A. D. I. M. S., & Itriyani, D. A. N. R. I. F. (2024). Sintesis Karbon Aktif dari Kulit Manggis (Garcina Mangostana) dengan Aktivator Kalium Hidroksida (KOH) sebagai Adsorben untuk Reduksi Biological Oxygen Demand (BOD) dan Chemical Oxygen Demand (COD) pada Limbah Cair Industri Tahu. *Seminar Nasional Kimia 2024 UIN Sunan Gunung Djati*.

Wismayanti, D., Diantariani, N., & Santi, S. (2015). Pembuatan Komposit ZnO-Arang Aktif Sebagai Fotokatalis Untuk Mendegradasi Zat Warna Metilen Biru. *Jurnal Kimia*, *9*(1), 109–116.

Wu, Z., Zhang, H., Ali, E., Shahab, A., Huang, H., Ullah, H., & Zeng, H. (2023). Synthesis of Novel Magnetic Activated Carbon for Effective Cr (VI) Removal Via Synergistic Adsorption and Chemical Reduction. *Environmental Technology and Innovation*, *30*, 103092.

Yuan, X., Cho, M., Lee, J. G., Choi, S. W., & Lee, K. B. (2020). Upcycling of Waste Polyethylene Terephthalate Plastic Bottles Into Porous Carbon for CF_4 Adsorption. *Environmental Pollution*, 114868.